Nonlinear vortex trail dynamics

Chjan C. Lim
Mathematics Department, University of Michigan, Ann Arbor, Michigan 48109
Lawrence Sirovich
Division of Applied Mathematics, Brown University, Providence, Rhode Island 02912

(Received 28 August 1987; accepted 11 December 1987)

The nonlinear evolution of periodic disturbances on vortex trails is considered. In addition to following small initial perturbations, large amplitude initial disturbances of the vortex trails are also studied. It is shown that the equations support a rich variety of essentially nonlinear solutions including unbounded and quasisteady ones. These solutions are found to correspond to various modes of vortex clustering in the physical plane. At the close of the paper, comparisons of these results with recent numerical and experimental findings on the wakes behind stationary cylinders, and also transversely oscillating bluff objects, are made.

I. INTRODUCTION

The von Karman model[1,2] differs in essential ways from the true physical situation (cf. Fig. 1). It is infinite in extent whereas a true wake is bounded by the body that generates the vortices. Also, viscosity does not figure in von Karman's model. As a remedy to this, recent inviscid models replace the vortex by a core of constant vorticity. However, as Meiron *et al.*[3] and Kida[4] have shown, this does not change the basic stability properties in any significant way. Moreover, the von Karman model shares many qualitative and quantitative features with the actual physical situation and its further study is therefore warranted (cf. Refs. 5–8).

We will show that the von Karman model gives rise to a rich and highly nonlinear variety of related solutions. Some of these solutions can be shown to evolve from the von Karman trail. Others are quasisteady spatially periodic arrays that result from the interaction of infinite rows of vortices. The latter class of solutions differ in an essential way from the von Karman trail but are nonetheless physically interesting and relate to certain experimental situations.[9,10] We also consider the effects of changing the aspect ratio on the evolution of the von Karman trails. Unlike the von Karman trail, the solutions we obtain are dynamic, i.e., they exhibit temporal behavior such as quasiperiodicity on one hand and unbounded motion on the other.

In this paper we describe a framework for solving periodic problems of the von Karman model. In particular it is shown that period-2 (four-group) disturbances are the most unstable (see Fig. 2) and hence of greatest interest. For this reason attention is focused on the four-group periodicity. No claim is made that, after instability is well advanced, the four-group is actually maintained in the physical situation, though Koochesfahani[9] has experimentally observed four-group periodicity for sustained periods of time. The results of extensive computer experiments on the equations of motion (13) form the main part of this paper. We believe that these results add more support to the physical relevance of the von Karman model, and at the close of this paper we attempt to relate our results to recent experimental and computational work.

II. KOCHIN'S EQUATIONS

The stability and evolution of periodic disturbances of two parallel rows of vortices can be formatted in terms of equations describing the interaction of many parallel rows, each containing an infinitude of vortices.[11] For example, a disturbance that is N periodic requires $2N$ equations. A sketch of this idea is shown in Fig. 1. The governing equations for N-periodic or $2N$-group problem are given by[11]

$$\frac{d\bar{Z}_k}{dt} = \sum_{j=1}^{2N}{}'(-1)^j \frac{\kappa}{2Nli} \cot\frac{\pi}{Nl}(Z_k - Z_j), \quad k = 1,\ldots,2N, \tag{1}$$

where a prime denotes exclusion of the term $j = k$ in the sum. Here, Z_k denotes the location of a typical vortex in the k th row. Odd numbered rows arise from the upper row in the original array and even numbered rows from the lower row.

We recall that only the von Karman case, for which the spacing ratio $k = h/l$ takes the value

$$k_0 = (1/\pi)\sinh^{-1}(1) \approx 0.281, \tag{2}$$

is not linearly unstable. In what follows, we do not restrict our study to this case. Since Kochin's derivation of (1) does not require the periodic disturbances to be small, these equations are well suited to the study of vortex configurations that are essentially large perturbations of the original array. We are interested not only in the evolution of the von Karman street but also in the existence of quasisteady spatially periodic configurations that do not evolve from the von Karman trails.

The four-group ($N = 2$) case is both the simplest and the most basic in the sense that a period-2 disturbance also has periods $2M$ for positive integer M. However, a more important reason for studying the four-group case is that linear stability theory implies it is the most unstable disturbance when the spacing ratio k is close to the special value k_0. This is shown in the Appendix.

Henceforth, we focus on the four-group case. For $N = 2$, the row equation (1) becomes

 0031-9171/88/050991-08$01.90

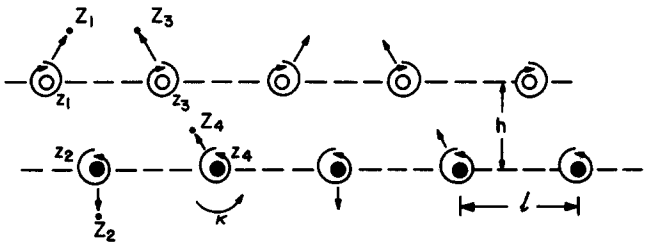

FIG. 1. The von Karman trail. Here h denotes the separation between rows, l denotes the distance between vortices in each row, and κ denotes the circulation of the vortices. Here and in Fig. 3, we adopt the convention that open circles represent negative circulation and filled circles positive circulation. Periodic disturbances of an equilibrium trail can be viewed in terms of the motion of parallel rows of vortices, capital Z's. The two-periodic or four-group case is shown.

$$\frac{d\bar{z}_k}{d\tau} = -i \sum_{j=1}^{4}{}'(-1)^j \cot(z_k - z_j) \tag{3}$$

in terms of the dimensionless variables

$$z_k = \pi Z_k/2l, \quad \tau = \pi\kappa/8l^2. \tag{4}$$

Symmetries allow these equations to be considerably reduced. It is clear that they can be rewritten as three complex equations in terms of differences only and, from (3), it follows that

$$C = z_1 - z_2 + z_3 - z_4 \tag{5}$$

is an invariant. Hence (3) reduces to two complex ordinary differential equations.

We pause to consider the physical significance of the invariant C. In general, $C = 2(z_1 - z_2)$ for an equilibrium vortex trail. Thus in complex notation, the invariant C takes the form

$$C = f + i\pi k, \tag{6}$$

where the *stagger* f is the dimensionless horizontal separation

$$f = \mathrm{Re}[\pi(Z_1 - Z_2)/l] \tag{7}$$

between the two rows in a vortex trail while the *aspect ratio* k is the dimensionless vertical separation

$$k = \mathrm{Im}[(Z_1 - Z_2)/l]. \tag{8}$$

For the perfectly staggered von Karman trail at special spacing ratio, $k = k_0$ (which we term the von Karman case), C has the value

$$C_0 = \pi(\tfrac{1}{2} + ik_0). \tag{9}$$

Given any assembly of four vortex rows, $\{z_1,z_2,z_3,z_4\}$ with a fixed value of C, it is easy to show that there is a corresponding equilibrium with the same value of C.

As discussed, periodic disturbances of the von Karman trail can be treated as the motion of parallel vortex rows. To relate the assembly of four rows $\{z_i\}$ to the evolution of an equilibrium vortex trail, we consider perturbations from the equilibrium configuration $\{z_i^e\}$, *which has the same value of* C. For example, if the assembly of four rows being considered has a C that differs from C_0 [Eq. (9)], the above procedure redefines the equilibrium state so that

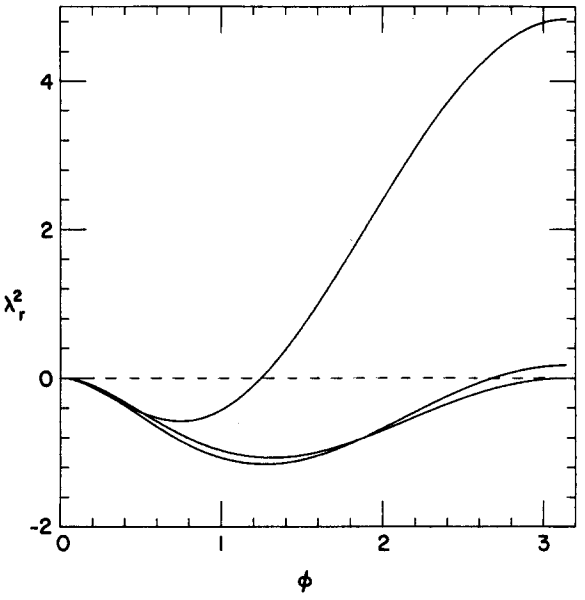

FIG. 2. Growth rates. The quantity $\lambda_r^2 = a^2 - c^2$ is plotted against the wavenumber ϕ from 0 to π. When $\lambda_r^2 > 0$, there is growth. The three curves represent values of the aspect ratio, $k = k_0$,0.3,0.4.

$$\Delta C = \sum_{i=1,3}(z_i - z_i^e) - \sum_{i=2,4}(z_i - z_i^e) = 0. \tag{10}$$

With this equilibrium as a starting point, we define normalized perturbations as follows:

$$\rho_k = z_k - (z_k^e + \bar{V}\tau), \tag{11}$$

where $\bar{V}$ is the velocity of the equilibrium trail. The governing equations for these perturbations (which can be arbitrarily large), in terms of the differences

$$\alpha = 2(\rho_2 - \rho_1), \quad \beta = 2(\rho_2 - \rho_3), \tag{12}$$

then take the form[11]

$$\begin{aligned} \frac{d\bar{\alpha}}{d\tau} &= -4i \sin\beta \left(\frac{1}{\cos\alpha + \cos\beta} - \frac{1}{\cos\beta + \cos C} \right), \\ \frac{d\bar{\beta}}{d\tau} &= -4i \sin\alpha \left(\frac{1}{\cos\alpha + \cos\beta} - \frac{1}{\cos\alpha - \cos C} \right), \end{aligned} \tag{13}$$

where C is the above invariant [Eq. (5)]. In terms of the distribution of vortices in the physical plane, the variable α denotes the change in the separation between the Z_2 and Z_1 rows, while β denotes the same for the Z_3 and Z_2 rows. Other changes in separations, e.g., $(\rho_3 - \rho_4)$, can be obtained from α and β and the equation

$$\rho_1 - \rho_2 + \rho_3 - \rho_4 = 0,$$

which is a consequence of (10). Kochin[11] derived (13) for the perfectly staggered case, $f = \pi/2$. We have extended this derivation to the general case of arbitrary four rows. Henceforth, we refer to (13) as Kochin's equations.

These equations may be put in Hamiltonian form,

$$\frac{d\bar{\alpha}}{d\tau} = -2i\frac{\partial H}{\partial \beta}, \quad \frac{d\bar{\beta}}{d\tau} = -2i\frac{\partial H}{\partial \alpha}, \tag{14}$$

where

$$H = -4\ln\{[(\cos\alpha - \cos C) \times (\cos\beta + \cos C)]/(\cos\alpha + \cos\beta)\}. \quad (15)$$

The constant C [Eq. (5)] represents two integrals of (3). As one can easily show $R_e H$ is an invariant of (14) and hence also of (3). Since (14) has two degrees of freedom and no apparent additional invariant, we conjecture that, except in special cases, the system is nonintegrable. This naturally brings up the question of whether (14) supports chaotic behavior. In spite of extensive computer experiments we could not uncover a single obviously chaotic case. In this paper, we discuss only regular behavior.

III. PROPERTIES OF KOCHIN'S EQUATIONS

In the von Karman case, where the aspect ratio $k = k_0$, the expression $\cos C$ in (13) becomes

$$\cos C = -i$$

and the original form of Kochin's equations is obtained[11]:

$$\frac{d\bar{\alpha}}{d\tau} = -4i\sin\beta\left(\frac{1}{\cos\alpha + \cos\beta} - \frac{1}{\cos\beta - i}\right),$$
$$\frac{d\bar{\beta}}{d\tau} = -4i\sin\alpha\left(\frac{1}{\cos\alpha + \cos\beta} - \frac{1}{\cos\alpha + i}\right). \quad (16)$$

We discuss symmetry and singularity properties of Kochin's equations in terms of (16) but most properties are similar in the general case (13).

Inspection shows that (16) is invariant under the transformation

$$\beta \to \alpha + \pi, \quad \alpha \to \beta - \pi. \quad (17)$$

Thus if $[\alpha(\tau),\beta(\tau)]$ is a solution, then $[\beta(\tau) - \pi, \alpha(\tau) + \pi]$ is also a solution. Further, the trigonometric form of Kochin's equations implies that the dependent variables have a basic periodicity of 2π. Thus we may restrict attention to the four space cylinders, $-\pi \leqslant \mathrm{Re}\,\alpha, \mathrm{Re}\,\beta \leqslant \pi$ (which itself is a consequence of the spatial periodicity of the rows of vortices). Another noteworthy property is *time symmetry*. Since

$$\tau = \pi\kappa t/8l^2$$

integrating the equations backwards in time can be accomplished by reversing the circulation κ and integrating forward in time.

Turning next to the critical points, we observe that Eqs. (16) have only one equilibrium point (modulo 2π), namely,

$$(\alpha,\beta) = (0,0). \quad (18)$$

This corresponds to the unperturbed trail in this case. Of importance is the observation that Eqs. (16) are singular if any of the following conditions are met:

$$\cos\alpha + i = 0 \Rightarrow \alpha = \pm(\pi/2 + i\pi k_0) = \pm\alpha_0, \quad (19)$$
$$\cos\beta - i = 0 \Rightarrow \beta = \pm(\pi/2 - i\pi k_0) = \pm\beta_0, \quad (20)$$
$$\cos\alpha + \cos\beta \Rightarrow \alpha_1 = \pm\beta_1 + (2n+1)\pi, \quad n \text{ an integer}. \quad (21)$$

[From (17) we see that (19) and (20) are essentially the same.] The last condition, (21), defines a two-dimensional manifold in the four-dimensional phase space of solutions.

The singularities (19)–(21) (and their variations) play a basic role in our work and we contend that they are significant in the experiment. We therefore detail their appearance in the physical plane in a case by case manner:

Case 1: ($\alpha = \pm\alpha_0$, $\beta \neq \pm\beta_0$). Two rows of opposite circulation merge into *vortex couples*; the other pair of rows remain apart. For a sketch of this situation, see Fig. 3(a). [This case includes the cases where $\beta = \pm\beta_0$ and $\alpha \neq \alpha_0$ by virtue of (17).]

Case 2: ($\alpha = \pm\alpha_0$, $\beta = \pm\beta_0$). Three rows merge into *vortex triplets* while the fourth vortex row stands alone.

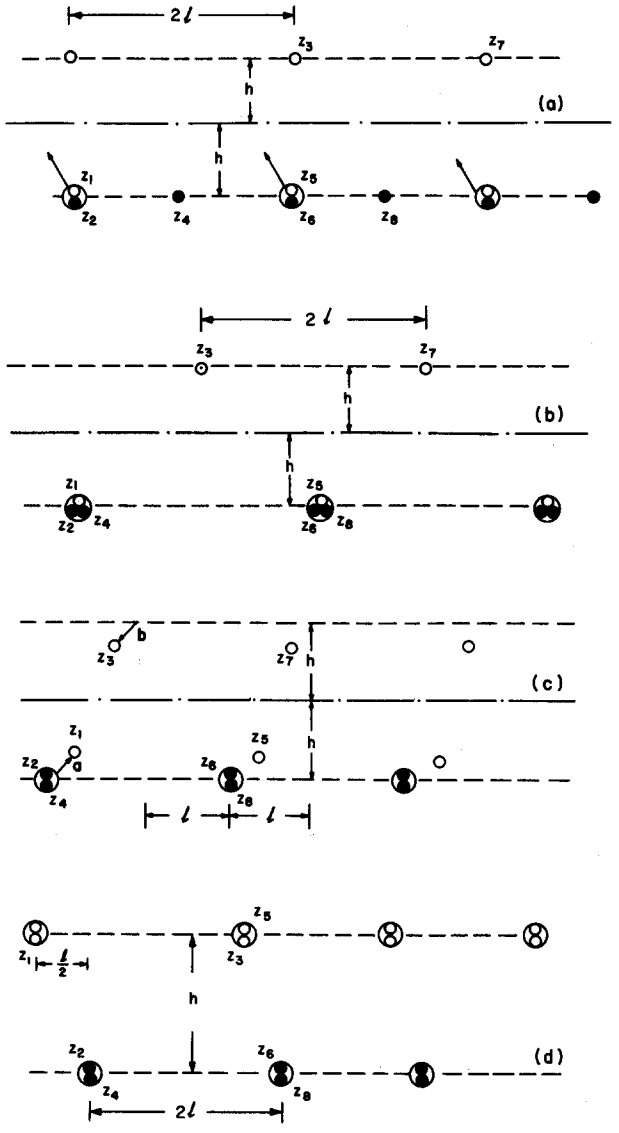

FIG. 3. Couples. (a) Two rows of opposite circulation merge into vortex couples while the remaining two rows remain apart. The resulting vortex couples have a relatively large velocity (denoted by the arrow) causing them to leave the trail. (b) Vortex triplets and doubling of linear dimensions. Three rows merge to form vortex triplets. Together with the isolated row, this forms a new perfectly staggered vortex trail with twice the length scales. (c) Vortex merging—pairs. Only vortices in one of the rows merge to form vortex pairs, e.g., (Z_2,Z_4). Vortices from the other row are sufficiently near these pairs to form loosely bound vortex triplets, e.g., Z_1 and (Z_2,Z_4). (d) Vortex pairs and staggered arrays with smaller aspect ratio. Vortices in both rows of the original trail merge to form vortex pairs. The resulting trail is staggered and has aspect ratio, $k' = 0.5k_0$.

This results in a new array with a doubling of the linear dimensions, see Fig. 3(b).

Case 3: ($\alpha = \alpha_1$, $\beta = \beta_1$). At least one imaginary part of α_1 or β_1 is nonzero. Two rows with the same circulation merge into *vortex pairs* while the other two rows are separated. For a sketch of this situation, see Fig. 3(c).

Case 4: The imaginary parts of α_1 and β_1 are zero, i.e., $\alpha_1 = m\pi$, $\beta_1 = n\pi$, where m,n are integers. Two *vortex pairs* result from the merging of similar vortex rows. This situation is shown in Fig. 3(d).

These four cases [modulo 2π and (17)] cover all possible singularities of (13) and therefore describe all possible ways that four vortex rows merge. We note, however, that these singular phase points cannot lie on trajectories of (13) because the Hamiltonian (15) tends to infinite values at these points. In particular, there are no orbits connecting the equilibrium point (18) where the Hamiltonian is finite and any of the above four types of singular points. Nonetheless, the behavior of Kochin's equation *near* these singularities is fundamental.

IV. NUMERICAL RESULTS

It is of interest to study the evolution of the slightly perturbed von Karman trail since such trails are *always unstable.*[11] A second goal is to find and classify bounded quasiperiodic solutions of (16) that do not evolve from the von Karman trails. Solutions in the (α,β) plane are discussed first and their corresponding arrangements in the physical plane are then given. In order to highlight the relative motion of the vortices, a set of *time frames* or *snapshots* of the solution is depicted in each case. In all the cases discussed, the time step in the Runge–Kutta scheme used for integrating (16) is selected to be small enough so that the relative change in the Hamiltonian, (15), remains less than 0.5%.

A. Collision of two vortex trails

First we consider small departures from the von Karman trail at the special spacing ratio k_0. A typical plot of (α,β) versus time τ is given in Fig. 4. Our numerical experiments show that only one of the variables α and β ultimately rises linearly in time. Prior to this we typically see the vibrations depicted in Fig. 4.

The corresponding situation in the physical plane is presented in a sequence of *snapshots in time.* In Fig. 5 and all subsequent time frames, the squares and diamonds represent vortices of the same negative circulation while octagons and stars depict vortices of positive circulation. The use of the four shapes is for identification purposes. The second frame in Fig. 5 represents the initial perturbation from the von Karman trail. In the third frame, the perturbation has grown and in the fourth frame, the vortex trail has separated into different (essentially noninteracting) trails moving laterally away from each other.

This sequence of events suggests that we describe the asymptotic behavior in terms of the *collision of two vortex trails.* Since Eqs. (16) are reversible, unbounded solutions can be *retraced* to $\tau = -\infty$. This is shown in the first frame of Fig. 5. Only at such times when α and β are $O(1)$ does full

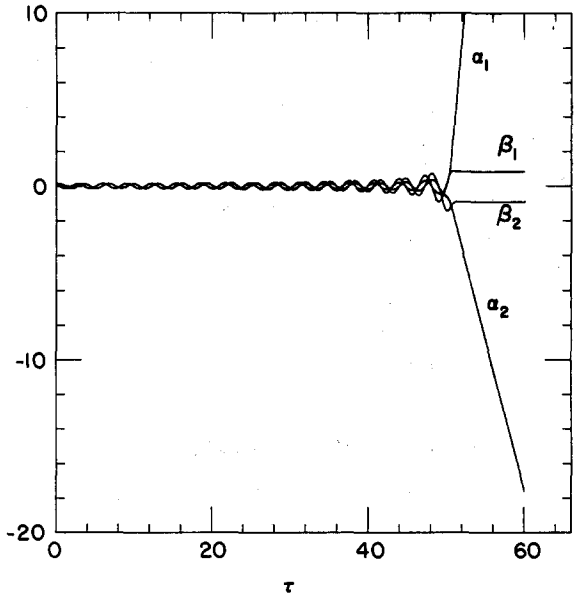

FIG. 4. Unbounded solution. A period of slowly growing oscillations around the equilibrium point leads to unbounded motion where the real and imaginary parts of α grow linearly while β tends to a constant. The subscripts 1 and 2 denote real and imaginary parts, respectively.

interaction between the four rows take place. Figure 5 depicts a *scattering* in which the two colliding trails exchange rows. The squares and stars are paired before the interaction but, after scattering, the squares are paired with octagons. Scattering in which the two trails pass through one another without row exchanges can also take place.

B. Quasisteady vortex clusters

A larger class of phenomena is observed if we consider initial data for (16) that are *not* constrained to be small perturbations. In addition to unbounded solutions, we also find quasiperiodic motion. One such set of unbounded solutions involves the formation of *vortex couples* from *triplets.* The triplet configuration that corresponds to a neighborhood of the case 2 singularity is unstable. Here, we give a numerical example of such an instability, in which two vortex rows of opposite circulations form a couple within the original cluster of three rows and diverge from the trail. Three time frames of the evolution of triplets into vortex couples are shown in Fig. 6. We note that such vortex couples are associated with the case 1 singularities of Eqs. (16).

The quasiperiodic motions of (16) appear to be of *three* basic types. One class has solutions exemplified by the plots in Fig. 7(a) of (α,β) versus time. Inspection of this figure indicates that there are two relatively close frequencies in the solutions. It shows a solution that remains near a case 2 singularity

$$(\alpha_0,\beta_0) = (\pi/2 + i\pi k_0, \pi/2 - i\pi k_0).$$

Our results imply that there is a fairly large set of such quasiperiodic orbits near a case 2 singularity. In addition, these solutions are also found at distances bounded away from the singularity, i.e., this is a global phenomena. In the physical

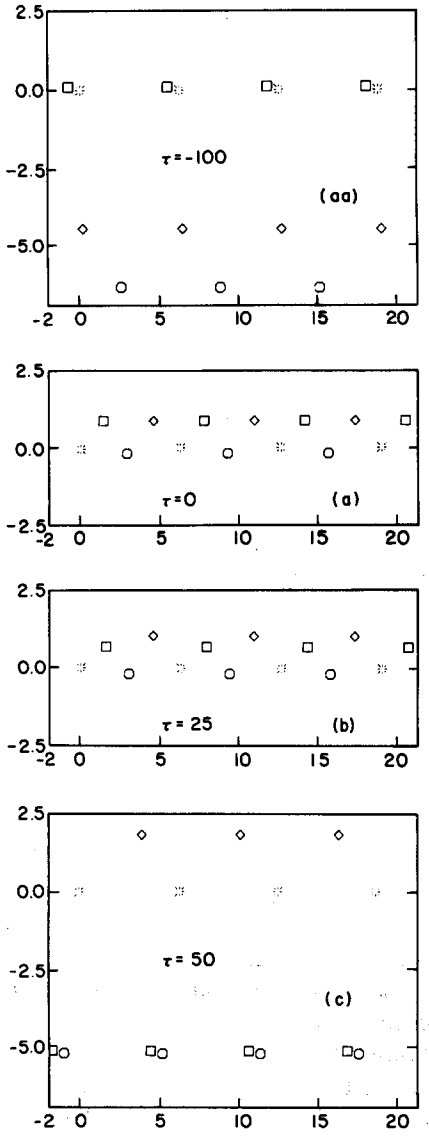

FIG. 5. Scattering of vortex trails. The relative motion of four vortex rows in the physical plane for the unbounded solution in Fig. 4 is shown. The initial perturbation of the vortex trail is given in frame 2. Frame 1 shows the configuration at $\tau = -100$ while frames 3 and 4 are for $\tau = 25$ and 50, respectively. Here, and in the following snapshots, the squares and diamonds represent vortices of negative circulation and the octagons and stars positive circulation, all of equal magnitude. The four shapes are necessary for identification purposes.

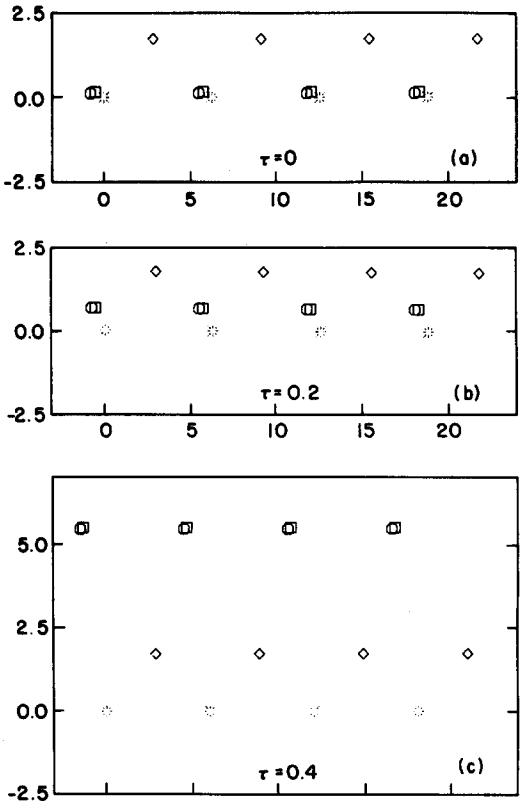

FIG. 6. Triplets to vortex couples. This illustrates the instability of the vortex triplet. It divides into a vortex couple and another row which then separate. Three frames of the process at $\tau = 0.0, 0.2, 0.4$ are shown.

plane, such bounded solutions correspond to high-frequency oscillations within a cluster of three vortex rows and an isolated fourth row. This is our first example of quasisteady vortex clusters. An important feature of these solutions is that the cluster of three vortices and the fourth vortex row constitute a new array for which the length scales are two times those of the original von Karman trail. This is depicted in Fig. 3(b).

The second class of quasiperiodic solutions remains close to the manifold of singularities given by (21). As can be seen in Fig. 7(a), where a time history of (α_r, β_I) is plotted, these solutions have two frequencies of which the ratio (or rotation number) is large. This intermediate situation related to case 3 singularities arises when a pair of *similar* vortex rows are relatively close together within a loose cluster of three rows. As the third vortex row in the cluster rotates around the *vortex pair*, it is brought alternately toward and then away from the fourth row in the configuration. This results in a vortex trail with changing stagger and aspect ratio. Since the velocity of a vortex trail depends on these quantities, the resulting vortex trail oscillates vertically. This is illustrated in Fig. 8. This is an example of loosely bound vortex clusters of three vortices.

By changing the separation between the third vortex and the vortex pair in the cluster, we obtain solutions that exhibit intermittency. Figure 9 illustrates the situation that arises when the third vortex (of opposite circulation) in the cluster is moved progressively away from the vortex pair. In each row of the original vortex trail, vortices repeatedly merge and separate, giving rise to intermittent *vortex pairs*. The vortices from one row migrate over to the other row and merge with vortex pairs of opposite circulation, forming intermittent *vortex triplets*. As these vortex pairs and triplets form and disperse, the effective stagger and aspect ratio of the resulting vortex trail changes in a repetitive way. Hence like the case before, these trails oscillate vertically. These solutions remain near the singular manifold (21) but wander (intermittently) close to the case 4 singularities, which are isolated points on this manifold (21).

The third class of quasiperiodic solutions is found in the neighborhood of case 4 singularities, e.g., $(\alpha_1, \beta_1) = (\pi, 0)$. Like the previous cases, they have two basic frequencies. In the physical plane, vortices in each row merge to form stable

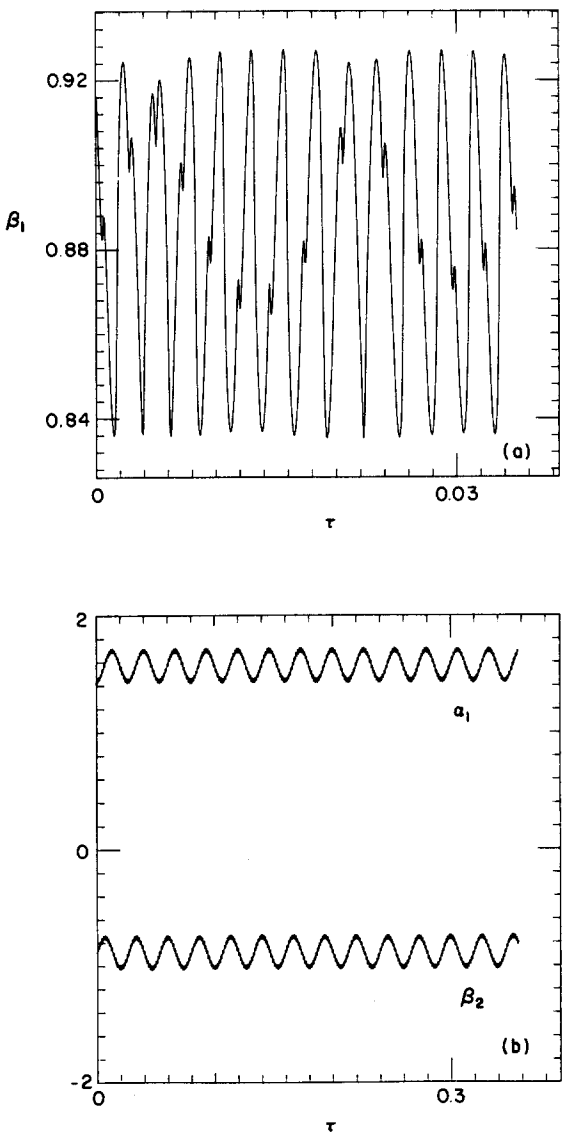

FIG. 7. (a) Quasiperiodic solutions I. Only the β variable is shown in the interest of simplicity. The oscillations are centered at a case 2 singularity, e.g., (α_0,β_0). In this case, there appear to be two basic frequencies. (b) Quasiperiodic solutions II. The real part of α and imaginary part of β are shown. The oscillations are close to case 3 singularities, and there appear to be two frequencies. The ratio of these frequencies is large.

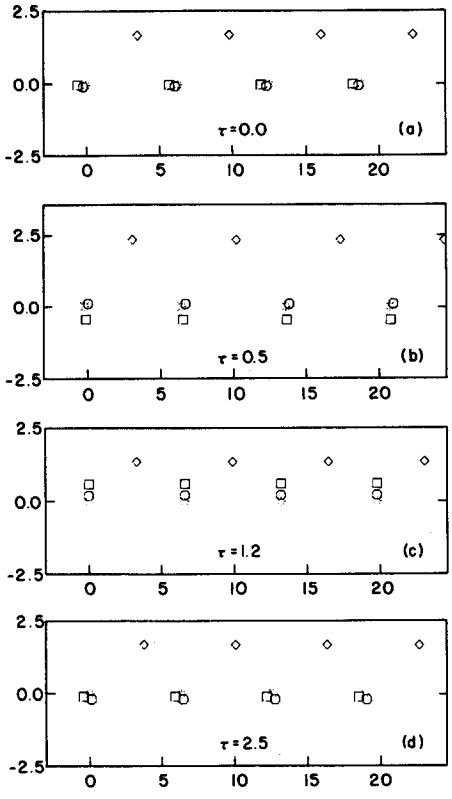

FIG. 8. Vortex pair within a triplet. Four frames of the periodic motions at $\tau = 0,0.5,1.2,2.5$ are shown.

rotating pairs. The resulting trail has an aspect ratio equal to about half the original value k_0. This is illustrated in Fig. 10.

From the above discussion, it is clear that *vortex couples* play a major role in the unbounded states encountered in the breakdown of the von Karman trails. Meanwhile *vortex pairs* and *triplets* are clusters that play important roles in the bounded recurrent states, which *do not* evolve from the von Karman trail. In performing the above numerical experiments, we have obtained detailed information on the phase flow of (16) in the neighborhood of singular points. This has confirmed the existence of several families of quasisteady spatially periodic vortex clusters in the dynamics of vortex rows.

C. The case $k \neq k_0$

In the above discussion only the von Karman case, i.e., $k = k_0$, is examined. Here we briefly consider the effects of changing the aspect ratio of the vortex trail. As in the cases above, only perfectly staggered vortex trails are treated. Instead of Eqs. (16) we use the general equations (13) with several different values for the parameter C.

von Karman[1,2] showed that such trails are linearly unstable. Since we are interested in the asymptotic states of these trails, only small perturbations of size less than ten percent of the scale length l are considered. Unlike the von Karman case ($k = k_0$, where small perturbations always lead to unbounded solutions), for $k > k_0$, small perturbations evolve into a wider class of solutions that includes bounded recurrent motions. For *intermediate values of* $k > k_0$, the numerical results indicate that small perturbations evolve into a dynamic state where vortex pairs and triplets form and disperse before becoming unbounded later. When *k is much larger than k_0*, the motions that result from small perturbations appear to remain in the finite part of the plane. These motions resemble some of the cases that result from large perturbations of the von Karman case, e.g., Figs. 8 and 9. Like their counterparts for $k = k_0$, the main features in these solutions are the repetitive formation and destruction of vortex pairs and triplets. Furthermore, there appears to be continuous sliding motion between the rows of vortices.

When $k < k_0$, the vortex trail is more unstable in the sense that small perturbations become unbounded after a short period of vibration of the original trail. In the von Karman case, this period of vibration typically lasts for about ten units of the normalized time τ. For $k \leq k_0$, there appears to be only one type of asymptotic state, namely, unbounded solutions (cf. Figs. 4 and 5).

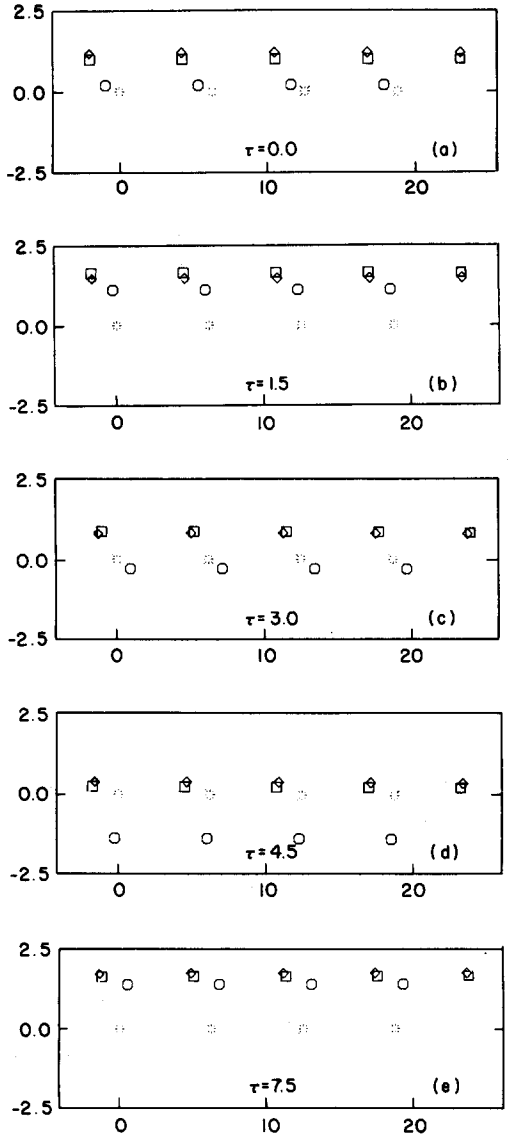

FIG. 9. Intermittent vortex pairs and triplets. Five frames of the process at $\tau = 0,1.5,3.0,4.5,7.5$ are shown. The configuration of the vortex trail alternates between triplets and pairs.

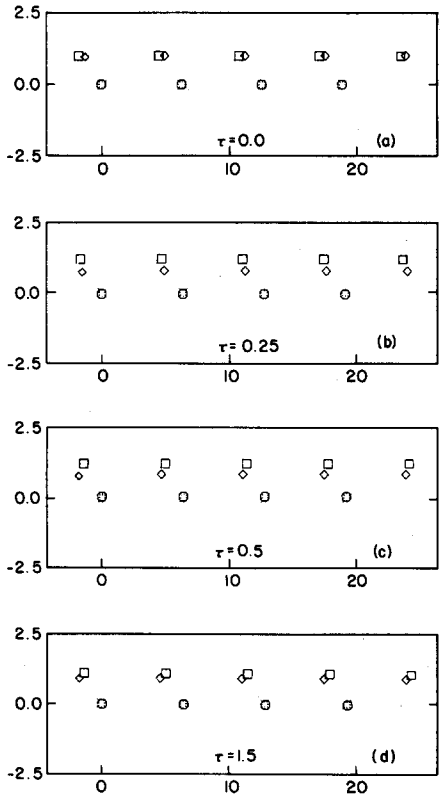

FIG. 10. Stable vortex pairs. Four frames of the process at $\tau = 0$, 0.25,0.5,1.5 are shown.

V. COMPARISONS WITH EXPERIMENTS

A. Wakes of bluff objects[17,18]

There are two experimental situations that can be compared with our numerical results. They are (i) the evolution and breakdown of the von Karman street generated by a stationary cylinder[12–16] and (ii) the quasisteady periodic arrays produced by strongly oscillating cylindrical objects.[9,10]

Taneda[12] reported that a secondary array of large eddies has been found in the far wake after the primary vortex trail has decayed. He advanced the hypothesis that these large eddies are caused by hydrodynamic instability of the wake profile. More recently Matsui and Okude[13] found similar arrays of large eddies with roughly twice the length scales of the primary vortex trail. They, however, believe that the large eddies result from the amalgamation of vortices in the primary trail. The phenomenon of vortex merging in the near wake (into clusters consisting of three vortices) has been reported by Basdevant, Couder, and Sadourny[14] at intermediate values of the Reynolds number. To this group of experimental results on the evolution of the von Karman street, we compare our numerical results on the evolution of the von Karman trails for $k > k_0$ (discussed in Sec. IV C). We recall that small perturbations generally suffice to produce vortex structures such as vortex pairs and triplets on von Karman trails if $k > k_0$. These solutions are inherently dynamic in that the vortex trails alternate between pairs and triplets (see Fig. 9). A shortcoming of this comparison is the inability to ascertain the average spacing ratio k in the experiments. It is generally known that the experimental value of k varies over a considerable range of about k_0.

Another phenomenon in the breakdown of the von Karman street behind a *fixed* cylinder is the formation of fast moving vortex couples[14,15] (of opposite circulation). We recall our numerical results from Sec. IV A: for von Karman trails with spacing ratio near k_0, small perturbations typically lead to unbounded solutions that consist of rapidly moving vortex couples (see Fig. 5). Numerical analogs of this phenomenon have also been obtained by Aref and Siggia.[17] More recently, Meiburg[18] reported similar results. These two works[17,18] use general vortex methods and are based on models that incorporate vortex cores. However, the above comparisons between our results and experiments and also with the numerical results[17,18] indicate that the point vortex model has physical relevance.

B. Wakes of oscillating cylinders

We now take up the comparison of our results from Sec. IV B with the second experimental situation. Koochesfa-

hani[9] and Williamson and Roshko[10] have reported on experiments where airfoils and cylinders are strongly oscillated in the transverse direction. They have found new periodic arrays with clusters of two or three vortices on one side and typically an isolated vortex on the other (see Fig. 7 in Ref. 9). These arrays are located immediately behind the oscillating cylinder and appear to persist downstream. It is clear from our analysis that these do not evolve from the von Karman trails.

We have found numerically three main families of bounded quasiperiodic solutions near the case 2, 3, and 4 singularities of Kochin's equations. These solutions consist of vortex clusters that oscillate about their centers. They typically persist for a relatively long time and we term this behavior quasiperiodic on the basis of the numerical evidence. For example, Fig. 8 illustrates periodic vortex clusters of three vortices while Fig. 10 depicts two rows of stable rotating vortex pairs.

Under different circumstances the von Karman model supports unbounded and quasiperiodic solutions, solutions that evolve from the equilibrium trail and solutions that do not. These solutions correspond to vortex structures in the physical plane that bear a resemblance to those found in two types of experiments.

ACKNOWLEDGMENTS

The authors take pleasure in acknowledging the unselfish help given to them by Tom Sharp in preparing the figures. They would like to thank Dr. M. Koochesfahani for helpful comments on the oscillating airfoil experiment.[9]

This work was supported by NASA under Grant No. 5-28547 and under the DARPA-URI Grant No. 5-28575.

APPENDIX: THE MOST UNSTABLE PERTURBATION

We demonstrate that the four-group case is the most unstable case. (This was also mentioned without proof by Meiron, Saffman, and Schatzman.[3])

The linearized theory of the Karman trail is governed by

$$\frac{d}{dt}\begin{bmatrix}\alpha\\ \beta\end{bmatrix}=\begin{bmatrix} ib & a-c\\ a+c & ib\end{bmatrix}\begin{bmatrix}\alpha\\ \beta\end{bmatrix},$$

where α and β are the generating functions for the perturbation quantities (see Refs. 5 and 6). The elements of the matrix are given by

$$a=\phi(2\pi-\phi)/2-\pi^2/\cosh^2 k\pi,$$

$$b=\pi\phi\sinh k(\pi-\phi)/\cosh^2 k\pi+\pi^2\sinh k\phi/\cosh^2 k\pi,$$

$$c=\pi^2\cosh k\phi/\cosh^2 k\pi-\pi\phi\cosh k(\pi-\phi)/\cosh k\pi,$$

where $k=h/l$ is the spacing ratio of the Karman trail. The eigenvalues of the above matrix are given by

$$\lambda=ib\pm\sqrt{a^2-c^2}.$$

Hence, there is exponential growth if (cf. Fig. 2)

$$\lambda_r^2=a^2-c^2>0.$$

At $\phi=0$,

$$a=-\pi^2/\cosh^2 k\pi,\quad c=\pi^2/\cosh^2 k\pi.$$

Therefore, $\lambda_r(\phi=0)=0$ for all k. On the other hand, at $\phi=\pi$,

$$c=0,\quad a=\pi^2/2-\pi^2/\cosh^2 k\pi\neq 0,\quad \text{if } k\neq k_0.$$

Therefore the growth rate for perturbations with wavenumber $\phi=\pi$, i.e., the four-group, is given by

$$\lambda_r=a.$$

Next, we note that there are only three stationary points for λ_r^2:

$$\frac{\partial\lambda_r^2(k,\phi)}{\partial\phi}=0\quad\text{at } \phi=0,\phi^*,\pi,$$

where ϕ^* is an intermediate value and depends on k. Taking the second partial derivative, we obtain

$$\frac{\partial^2(\lambda_r^2)}{\partial\phi^2}<0\quad\text{at } \phi=0,\pi,\quad\text{for } k \text{ near } k_0.$$

Therefore, we conclude that $\phi=0$ is a local maximum, $\phi=\pi$ is a global maximum for $\phi\in[0,\pi]$, and thus there is a maximum growth for the four-group perturbation if the spacing ratio k is near the special value k_0.

[1]Th. von Karman, Gottingen Nachrichten Math. Phys. Kl. **1911**, 509.
[2]Th. von Karman and H. Rubach, Phys. Z. **13**, 49 (1912).
[3]D. I. Meiron, P. G. Saffman, and J. C. Schatzman, J. Fluid Mech. **147**, 187 (1984).
[4]S. Kida, J. Fluid Mech. **122**, 487 (1982).
[5]L. Sirovich, Phys. Fluids **28**, 2723 (1985).
[6]L. Sirovich and C. Lim, in *Vortex Dominated Flows*, edited by M. Y. Hussaini and M. Salas (Springer, New York, 1986), p. 44.
[7]C. Lim and L. Sirovich, Phys. Fluids **29**, 3910 (1986).
[8]C. Lim and L. Sirovich, submitted to SIAM J. Appl. Math.
[9]M. M. Koochesfahani, AIAA-87-0111, 1987.
[10]C. Williamson and A. Roshko, Bull. Am. Phys. Soc. **31**, 1690 (1986).
[11]N. E. Kochin, I. A. Kibel, and N. V. Roze, *Theoretical Hydromechanics* (Interscience, New York, 1964).
[12]S. Taneda, J. Phys. Soc. Jpn. **14**, 843 (1959).
[13]T. Matsui and M. Okude, in *Proceedings of the Fifteenth International Congress of Theoretical and Applied Mechanics*, University of Toronto, 1980 (North-Holland, Amsterdam, 1980), p. 1.
[14]C. Basdevant, Y. Couder, and R. Sadourny, *Macroscopic Modeling of Turbulent Flows*, in Lecture Notes in Physics, Vol. 23 (Springer, Berlin, 1984), p. 327.
[15]Y. Couder and C. Basdevant, J. Fluid Mech. **173**, 225 (1986).
[16]J. Cimbala, H. Nagib, and A. Roshko, Bull. Am. Phys. Soc. **26**, 1256 (1981).
[17]H. Aref and E. Siggia, J. Fluid Mech. **109**, 435 (1981).
[18]E. Meiburg, J. Fluid Mech. **174**, 83 (1987).